Werk

Jahr: 1979
Kollektion: fid.geo
Signatur: 8 Z NAT 2148:46
Digitalisiert: Niedersächsische Staats- und Universitätsbibliothek Göttingen
Werk Id: PPN1015067948_0046
PURL: http://resolver.sub.uni-goettingen.de/purl?PPN1015067948_0046

LOG Id: LOG_0030
LOG Titel: Calculation of the effect of the oceans on geomagnetic variatons with an application to the Sq field during the IGY
LOG Typ: article

Übergeordnetes Werk

Werk Id: PPN1015067948
PURL: http://resolver.sub.uni-goettingen.de/purl?PPN1015067948
OPAC: http://opac.sub.uni-goettingen.de/DB=1/PPN?PPN=1015067948

Contact

Niedersächsische Staats- und Universitätsbibliothek Göttingen
Georg-August-Universität Göttingen
Platz der Göttinger Sieben 1
37073 Göttingen
Germany
Email: gdz@sub.uni-goettingen.de

J. Geophys. 46, 273–289, 1979

Journal of Geophysics

Calculation of the Effect of the Oceans on Geomagnetic Variations With an Application to the Sq Field During the IGY

B.A. Hobbs and G.J.K. Dawes

Department of Geophysics, University of Edinburgh, James Clerk Maxwell Building, Mayfield Road, Edinburgh EH9 3JZ, Great Britain

Abstract. A thin non-uniformly conducting shell at the Earth's surface is taken to represent the distribution of the world's oceans. The continents are represented by zero conductance. The Earth model is completed by a perfectly conducting conductosphere electrically insulated from the surface shell. The theory for electromagnetic induction in such a model has been given by Hobbs and Brignall (1976); this paper presents the detailed method of calculating solutions, using that theory. Examples of induction by various spherical harmonic terms are presented. A synthesis of such solutions is used to approximate the observed external Sq field during the IGY, and the corresponding calculated induced field in the model Earth is compared to that observed.

Key words: Electromagnetic induction – Oceans – Sq – Analytic continuation – Numerical calculations – Vertical component induction.

Introduction

The classical paper of Lahiri and Price (1939) showed that to model the response of the Earth to Sq and Dst variations requires the presence of a conductosphere, in which the conductivity increases steeply with depth, together with a thin conducting shell at the Earth's surface. One possibility is that this shell, taken to be uniform in their model, represents an approximation to the effect of the oceans. However, the oceans are distributed irregularly over the Earth's surface. To obtain a more detailed analysis of their effect on geomagnetic variations therefore requires solution to the problem of electromagnetic induction in a non-uniformly conducting thin shell. Price (1949) gave the appropriate theory and a slight extension, involving analytic continuation (Hobbs and Brignall, 1976) enables his basic theory to be used for general problems. The next step is to make numerical calculations for a conductosphere and oceanic shell in which the conductance of the shell is more representative of the

0340-062X/79/0046/0273/$03.40

ocean/continent distribution. That is the task of this paper. The model for the surface shell is shown in Fig. 1, and is described below. In this first investigation the conductosphere is assumed perfectly conducting. The region between the shell and conductosphere has zero conductivity.

The general method of solution and details of the numerical calculations are described in this paper and examples are given of induction by elementary spherical harmonic terms. Such harmonic terms can be superposed to obtain any inducing field and the corresponding solution may be determined. As an example, a study is made of induction by the Sq field during the IGY, as determined by Malin and Gupta (1977).

Mathematical Method

Since the surface shell is assumed infinitesimally thin the currents induced therein may be described by a current streamline function ψ. The boundary condition to be satisfied at the surface $r=a$ (Price, 1949) is

$$\operatorname{div}(\rho \operatorname{grad} \psi) = -\mu(\partial Z^e/\partial t) - \mu(\partial Z^i/\partial t) \tag{1}$$

where ρ is the reciprocal of the conductance of the shell, μ is the freespace permeability and $(\partial/\partial t)$ denotes differentiation w.r.t. time. For a conductosphere-shell model, Z^e and Z^i, both vertical fields measured positive down, have the following significance. A primary magnetic field external to the shell may be written as the gradient

$$\mathbf{H} = \operatorname{grad} \Omega^p$$

where Ω^p is the scalar magnetic potential. Only the radial component of this field has any induction effect since the model confines induced current flow to concentric shells. The vertical component of this primary inducing field is

$$Z^p = (\partial \Omega^p/\partial r). \tag{2}$$

This primary field induces current flow directly in the conductosphere and the magnetic field of these currents has a vertical component at $r=a$ which we denote by Z^c. The initial vertical field causing induction in the shell is then

$$Z^e = Z^p + Z^c. \tag{3}$$

Currents induced in the surface shell (and described by ψ) have a magnetic field the vertical component of which causes further induction in the shell (the self induction effect). In addition, the magnetic field due to ψ induces currents in the conductosphere, the magnetic field of these currents induces further current flow in the shell (the mutual induction effect). The vertical component of the magnetic field at the surface $r=a$ due to both self and mutual induction is denoted by Z^i. Thus the total vertical component at $r=a$ is

$$Z^{\text{tot}} = Z^e + Z^i, \tag{4}$$

the induced vertical component is

$$Z^{\text{ind}} = Z^c + Z^i. \tag{5}$$

For time-harmonic fields varying as $\exp(i\omega t)$ the operator $(\partial/\partial t)$ may be replaced by $i\omega$ where ω is angular frequency. Price (1949), shows that Eq. (1) may be solved by iteration, where for the first step Z^i is ignored, and for subsequent steps successive approximations to Z^i are used. This method yields a series solution for ψ of the form

$$\psi = \psi_0 + \psi_1 + \psi_2 + \ldots \tag{6}$$

which depends on frequency ω and converges for ω small.

It is convenient to define

$$\phi(\omega) = \frac{\psi}{\omega} = \sum_{j=0}^{\infty} \omega^j \phi_j \tag{7}$$

where $\omega^{j+1}\phi_j = \psi_j$ and ϕ_j is independent of frequency. For a given configuration of conductors, (7) is a Taylor series having a certain radius of convergence. Hobbs and Brignall (1976) show that analytic continuation may be used to determine a series for ϕ convergent for all real ω. The transformation required is

$$p = \omega/(\gamma - \omega) \tag{8}$$

for some constant γ. This yields the solution

$$\phi(\omega) = (\gamma/(\gamma - \omega)) \sum_{l=0}^{\infty} p^l \chi_l \tag{9}$$

where the χ_l's are the linear combinations

$$\chi_l = \sum_{j=0}^{l} \binom{l}{j} \gamma^j \phi_j. \tag{10}$$

The constant γ has an optimum value given by

$$\gamma = 1.14\, \Omega_1\, i \tag{11}$$

where Ω_1, the smallest eigenvvalue of (1), is

$$\Omega_1 = \lim_{j \to \infty} |\phi_{j-1}|/|\phi_j|. \tag{12}$$

$|\phi_j|$ is some norm of ϕ_j (Hobbs and Bringall, 1976, p. 535). With the functions $\{\phi_j\}$ known, series (9) is the solution of Eq. (1) for any real frequency ω.

The frequency independent functions ϕ_j are determined by the following 2-part iterative procedure. The first part of the j'th iterative step is the solution of

$$\operatorname{div}(\rho \operatorname{grad} \phi_j) = R_j \tag{13}$$

for ϕ_j, where R_j is known. The second part is the determination of R_{j+1} from ϕ_j. We define

$$\begin{aligned} R_j &= -i\mu Z^e \quad j=0 \\ &= -i\mu Z_j \quad j \geqq 1 \end{aligned} \tag{14}$$

where

$$Z^i = \sum_{j=1}^{\infty} \omega^j Z_j. \tag{15}$$

This second part is then accomplished by surface integral formulae for Z_j in terms of ϕ_{j-1} given by Hobbs and Price (1970) representing both self and mutual induction. Methods of numerical quadrature for these integrals is given in Hobbs (1971). It remains to solve, at each step, the differential Eq. (13).

A Finite Difference Approximation and Method of Solution

Equation (13) can be solved readily only for very simple distributions of ρ. We determine a numerical solution by replacing the differential equation with a finite difference form and solving the resulting linear system of equations. The discrete points at which values of ϕ_j are to be determined are defined as the intersections (nodes) of latitude and longitude lines, with some given spacing, on the surface $r=a$. In the present application, lines spaced every 5° in latitude and longitude are used, giving 2522 nodes. Each node of this grid is specified as an oceanic or a continental point, these being chosen by reference to world maps (taking into account continental shelves) with the constraint that, apart from Antarctica, there should be one continuous land mass. The conductance at the nodes corresponding to this land mass, and to Antarctica, are set to zero. Figure 1 is a Plate Carré projection of the surface shell in which adjacent nodes corresponding to zero conductance at the edge of land masses have been joined by straight lines. It roughly approximates the distribution of continents and oceans. Nodes for oceanic points are assigned an appropriate value of ρ.

In order to evaluate the r.hs. of Eq. (12) and to measure the accuracy of solutions, a norm $|\phi_j|$ has to be defined. For any function f having numerical values at the oceanic nodes, we choose

$$|f| = \{\Sigma'(f(\theta, \lambda))^2\}^{\frac{1}{2}} \tag{16}$$

where θ and λ are the co-latitude and longitude of a node respectively, and the sum Σ' extends over the 20 nodes indicated by circles in Fig. 1.

For each iteration, ϕ_j is chosen as zero on the continental mass and is a prescribed constant on Antarctica. (The method of determining this constant is given below under 'the island condition.') To find the remaining values of ϕ_j, Eq. (13) has to be discretized at each oceanic point and this is achieved by replacing 1st and 2nd derivatives of ϕ_j, and 1st derivatives of ρ, by their 3-point finite-difference approximations. For points adjacent to a boundary, these

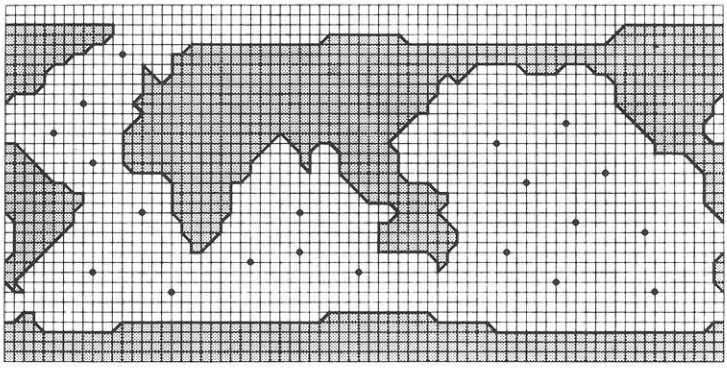

Fig. 1. Plate Carré projection of the surface shell representing the oceans and continents on a $5° \times 5°$ grid. Latitude span is from North to South poles. Longitude span is from 75° W *(left margin)* to 70° W *(right margin)*, an overlap of 5°. *Full circles* indicate nodes from which norms of solutions are calculated. The surface shell contains one mainland and one island

formulae apply directly to ϕ_j, whereas one-sided differences are used for the derivatives of ρ.

There are 1406 oceanic points in the approximation given by Fig. 1. A direct solution therefore requires inversion of a 1406×1406 matrix. The matrix is sparse, may be partitioned, and the partitioned matrices are either zero or striped. It is possible to invert such a matrix, but it is also amenable to iterative methods of solution. An adaptation of the block iterative method of Cuthill and Varga (1959) was used. A natural method of defining blocks is to consider them composed of all points on a given line of latitude between two coastlines. Inspection of Fig. 1 shows that the oceanic points may be represented by 76 such blocks, ranging in length from 1 to 72. To update the values of ϕ_j in a given block, the finite-difference approximation is applied, with the values of ϕ_j on adjacent lines of latitude and boundaries assumed known. The only inversion required is that of a simple tri-diagonal matrix. To avoid bias, the iterations commence with $\phi_j = 0$ in all blocks. Updating the 76 blocks in prescribed order corresponds to 1 iteration. The process is repeated until a given accuracy is achieved. In our numerical examples, the iterations were terminated when the norm $|\phi_j|$ changed from one iteration to the next by less than 0.1 %. (In some cases of slow convergence, 0.25 % was used as the terminating value).

The Island Condition

The current streamline function ψ is arbitrary to within a constant. We are at liberty therefore to choose the value of ψ on one coastline (and it will be the same value over that land mass). We choose the value $\psi = 0$ on the joined continents, but have to determine the constant value of ψ on Antarctica. For each 1st part of our 2-part iterative scheme, this means finding the constant value of $\phi_j = \phi_j^c$ on Antarctica and on its boundary. The value ϕ_j^c must be such

that the corresponding solution ϕ_j satisfies Faraday's law (in our frequency independent form)

$$\oint_\Gamma \rho\,\hat{\mathbf{r}} \wedge \nabla\phi_j \cdot \mathbf{dl} - i \iint_S \mathbf{B}_j \cdot d\mathbf{S} = 0 \tag{17}$$

where S is a surface that includes Antarctica and which is bounded by a curve Γ lying within the ocean. $\mathbf{B}_j \cdot d\mathbf{S}$ is the flux of magnetic induction passing through an element of the surface $d\mathbf{S}$ at the j'th iterative step. If S is part of the surface $r=a$ then

$$\mathbf{B}_j = \mu Z_j \hat{\mathbf{r}} \tag{18}$$

To find ϕ_j^c we solve Eq. (13) twice with two different boundary values ϕ_j^a and ϕ_j^b, and use the resulting solutions to determine $\mathscr{L}(\phi_j^a)$, $\mathscr{L}(\phi_j^b)$ where $\mathscr{L}$ is the value of the l.h.s. of Eq. (17). The value ϕ_j^c such that $\mathscr{L}(\phi_j^c)=0$ is found by the linear interpolation

$$\phi_j^c = \{\phi_j^a \mathscr{L}(\phi_j^b) - \phi_j^b \mathscr{L}(\phi_j^a)\}/\{\mathscr{L}(\phi_j^a) - \mathscr{L}(\phi_j^b)\}. \tag{19}$$

In the following calculations the boundary values $\phi_j^a = 1$, $\phi_j^b = -1$ were used. Solutions for the many island problem may be similarly constructed as outlined by Bullard and Parker (1970).

Final Solution and Accuracy

For a given configuration of conductors and for a given inducing field (usually in the form of a spherical harmonic of degree n, order m) the functions $\{\phi_j\}$ may be determined and stored. The solution for any frequency is then obtained using the series (9).

To measure the accuracy of a solution for a given inducing field and frequency, and thereby to determine the number of terms required in the sum (9), we re-write Eq. (1) as

$$L = R \tag{20}$$

where

$$L = \operatorname{div}(\rho \operatorname{grad} \psi) + i\omega\mu Z^i \tag{21}$$

and

$$R = -i\omega\mu Z^e. \tag{22}$$

R is given whereas L is determined by the solution. A measure of the accuracy of the solution is afforded by calculating

$$\varepsilon = (|L-R|/|R|) \times 100\,\% \tag{23}$$

where the norms are defined by Eq. (16). We continued adding terms in the sum (9) until ε no longer decreased (presumably because of round-off errors). The

solutions were generally accurate to 1% or less in about 8 iterations, although the last 3 or 4 of these iterations produced little improvement. The ratio of successive norms $|\phi_{j-1}|/|\phi_j|$ had reached a fairly steady value by this stage, so that γ (Eq. 11) was well determined. (In any case, the value of γ is not critical). Thus, as in the simple example considered by Hobbs and Brignall (1976), the series (9) is rapidly convergent and only a few terms, say 4 or 5, need be calculated for accurate solutions. Some examples of convergence are shown in Table 1 for the cases described below.

Numerical Values

The value of ρ for each oceanic point was taken as $0.625\ 10^{-4}$ ohm. This corresponds to an ocean of conductivity $4\,\mathrm{Sm}^{-1}$ and of depth 4 km. The conductosphere was assumed perfectly conducting and of radius $0.9\,a$, the Earth's radius a being $6.37\ 10^3$ km.

A General Inducing Field

Under the usual geomagnetic assumptions, an external varying magnetic field may be represented as the gradient of a scalar magnetic potential function Ω^p satisfying Laplace's equation. The general solution for Ω^p therefore consists of an infinite sum of spherical harmonics each of the form

$$\Omega_n^m(\omega) = a \left(\frac{r}{a}\right)^n \begin{Bmatrix} \cos m\lambda \\ \sin m\lambda \end{Bmatrix} P_n^m(\cos\theta) \exp(i\omega t). \tag{24}$$

Here the sphere of reference is the Earth's surface $r=a$, (r, θ, λ) are spherical polar coordinates and $P_n^m(\cos\theta)$ is the Schmidt partially normalised associated Lengendre polynomial of degree n, oder m. Any inducing field may be synthesised by an appropriate sum of functions (24) over n, m, and ω. As in Hobbs (1971) the normal component Z^e of the initial inducing field for the oceanic shell corresponding to the harmonic (24) is

$$Z^e = n(1-\zeta^{2n+1}) \begin{Bmatrix} \cos m\lambda \\ \sin m\lambda \end{Bmatrix} P_n^m(\cos\theta) \exp(i\omega t) \tag{25}$$

where $\zeta = b/a$ and b is the radius of the conductosphere.

We have solved the induction equation, and stored the solutions, for a large number of harmonics and are thus able to synthesise many inducing fields. For the Sq field, which is considered below, we have determined solutions corresponding to 16 harmonics, each solution having an in-phase and a quadrature part. The solutions are best displayed by contours on the surface $r=a$ of the current streamline function ψ, the vertical component Z^i and the total vertical component $Z^e + Z^i$. A complete description would thus require 80 diagrams. We give a few representative examples from this set. As the order n of the spherical harmonic increases, so does the value of Z^e in Eq. (25). The relevant coefficient

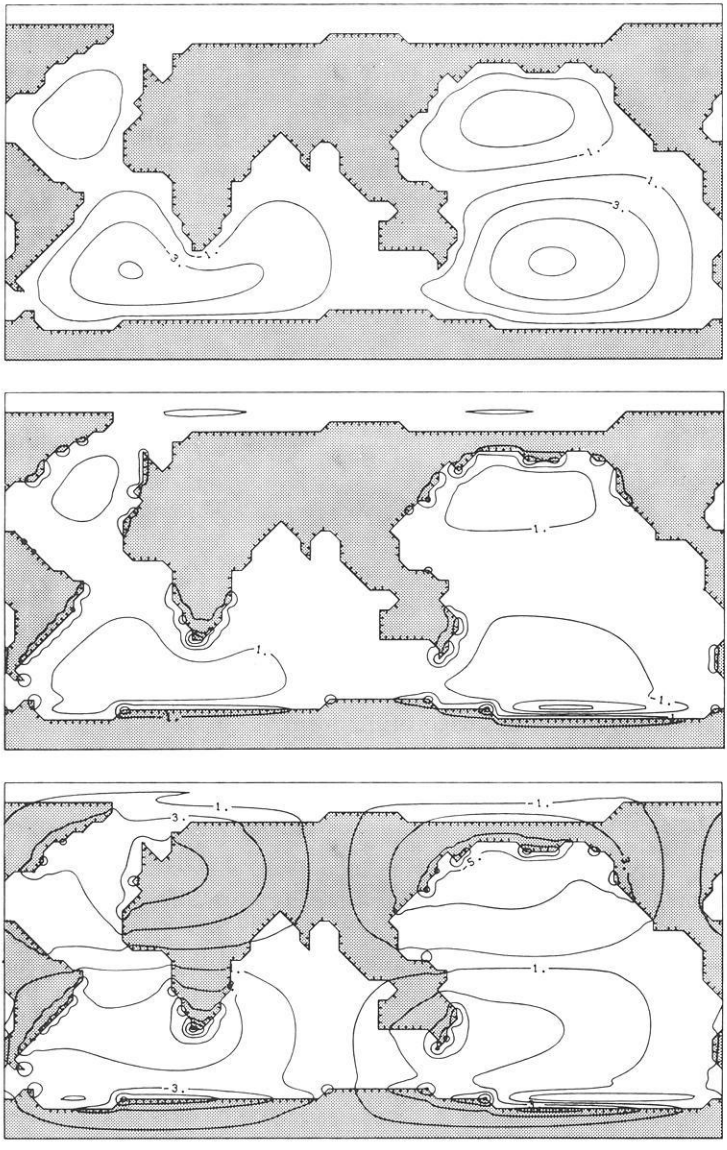

Fig. 2a–c. The in-phase part of the solution for induction by the unit amplitude harmonic $\cos\lambda P_2^1(\cos\theta)$ of period 24h. **a** Streamline function. 500A flows between adjacent contours, positive values indicate anti-clockwise flow. **b** Induced vertical field (positive down) in units of 0.125nT. Contour intervals are 0.25nT. **c** Total vertical field, units and intervals as in **(b)**

being $n(1-\zeta^{2n+1})$ times the normalisation coefficient for the harmonic. This increase is due partly to the spatial variation of the harmonic and partly to the influence of the conductosphere. The increase is notable in Figs. 2, 4, and 5. In specifying an inducing field, care must therefore be taken to ensure that all relevant harmonic terms, especially in the sum for Z^e, are accounted for.

Table 1. Details of the intermediate calculations for 3 spherical harmonic inducing fields

Harmonic Period	$\cos\lambda P_2^1(\cos\theta)$ 24h	$\sin 2\lambda P_3^2(\cos\theta)$ 12h	$\cos 3\lambda P_4^3(\cos\theta)$ 8h
(a) The ratio of successive norms $\lvert\phi_{j-1}\rvert/\lvert\phi_j\rvert$ *in units of* 10^{-4}Hz			
Iteration No.			
3	1.045	1.048	1.073
4	1.044	1.040	1.072
5	1.049	1.038	1.070
6	1.056	1.041	1.068
7	1.066	1.050	1.067
8	1.079	1.062	1.066
9	1.089	1.075	1.068
(b) The parameter ε *(an indication of* % *accuracy achieved)*			
Iteration No.			
3	1.952	1.562	1.613
4	1.313	1.180	0.677
5	0.967	1.021	0.452
6	0.860	1.003	0.399
7	0.824	1.000	0.384
8	0.693	0.983	0.376
9	0.414	0.964	0.373

Example: $\cos\lambda P_2^1(\cos\theta)$; In-Phase; Period 24 h

Figure 2a shows the current streamline function ψ for the above case. The time origin is at $\lambda = 180°$. In a uniform ocean the above harmonic would induce 4 current vortices with symmetry about $\lambda = 180°$ and anti-symmetry about $\theta = 90°$. Our model attempts to respond in that way, but the vortices are greatly distorted by the land masses. The vertical component Z^i is shown contoured in Fig. 2b. The field is practically zero over the continents, is small over oceans and has its largest values near coastlines. Physically, the induced currents are trying to flow so as to oppose the magnetic field over the oceans. The current gradient is steepest near the ocean edges, and this gives rise to large magnetic fields there. In Fig. 2c the induced and inducing fields are combined. Basically the pattern is that of 4 vortices, but these are somewhat distorted by the presence of the oceans. The effect of the non-uniform surface shell is to reduce the vertical field over the oceans and to distort it near ocean/continent boundaries. If the oceans were perfectly conducting (which is mathematically the same as the limit $\omega \to \infty$) the total vertical field over the oceans would be zero. For the real oceanic conductance and for a period of 24 h the solution is far from this limit. (Diagrams 4c and 5c show the effect of increasing frequency, Z^{tot} over the oceans being successively reduced compared to that over continents. The overall strength is increased however, owing to the increased spatial variation). It should be remembered that this simple cylindrical projection gives undue emphasis to points near the north and south poles, the field distortion near Antarctica is not as predominant as it appears in the diagrams.

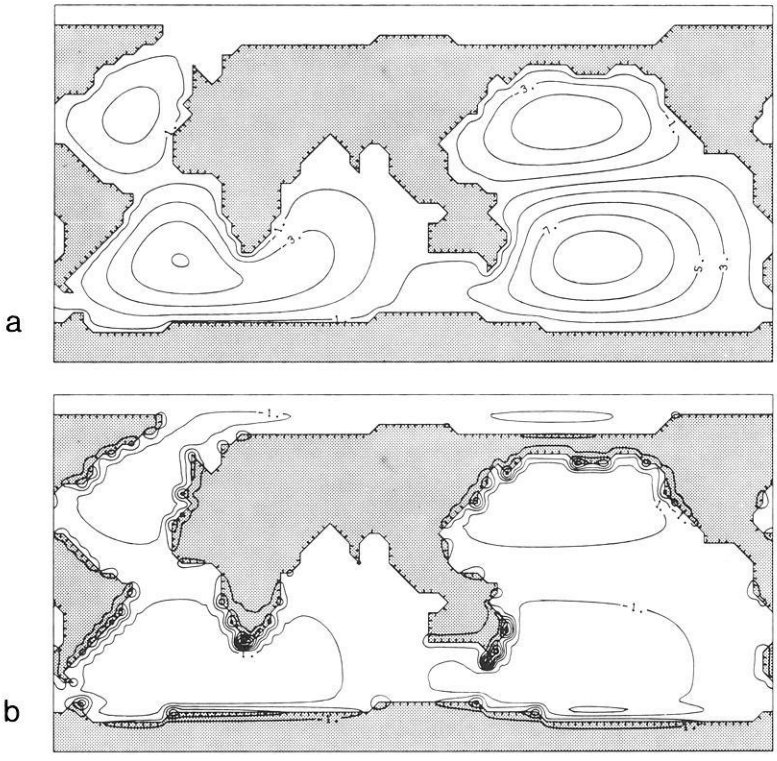

Fig. 3a and b. The quadrature part of the solution for induction by the unit amplitude harmonic $\cos\lambda P_2^1(\cos\theta)$ of period 24h. Contour values as in Fig. 2. **a** Streamline function, **b** induced vertical field

This solution was obtained in 9 iterations to within 0.414% as measured by ε in Eq. (23). Details of the intermediate calculations, in the form of the ratio of successive norms $|\phi_{j-1}|/|\phi_j|$ and the value of ε after each iteration are given in Table 1a and b for this harmonic and for the following examples. This solution could be obtained to within 1% in only 5 iterations.

In all the examples, the smallest eigenvalue is approximately $1.08\ 10^{-4}$ Hz. The implication is that the low frequency method resulting in series (6) is convergent for frequencies less than this value. In terms of period P series (6) is convergent for

$P > 16.2$ h.

This result is predicted approximately by the simple formula of Hobbs (1971) (inequality 20) which is dependent on spherical harmonic order n and which gives $P > 18.3$, 16.7, 15.2 h for orders $n = 2$, 3, 4 respectively.

Example: $\cos\lambda P_2^1(\cos\theta)$; Quadrature; Period 24 h

To complete the description of induction by the harmonic $\cos\lambda P_2^1(\cos\theta)$ the 2 diagrams for the imaginary parts of ψ and Z^i are given in Fig. 3a and b. The induced field in quadrature is seen to be more intense than that in-phase. Again

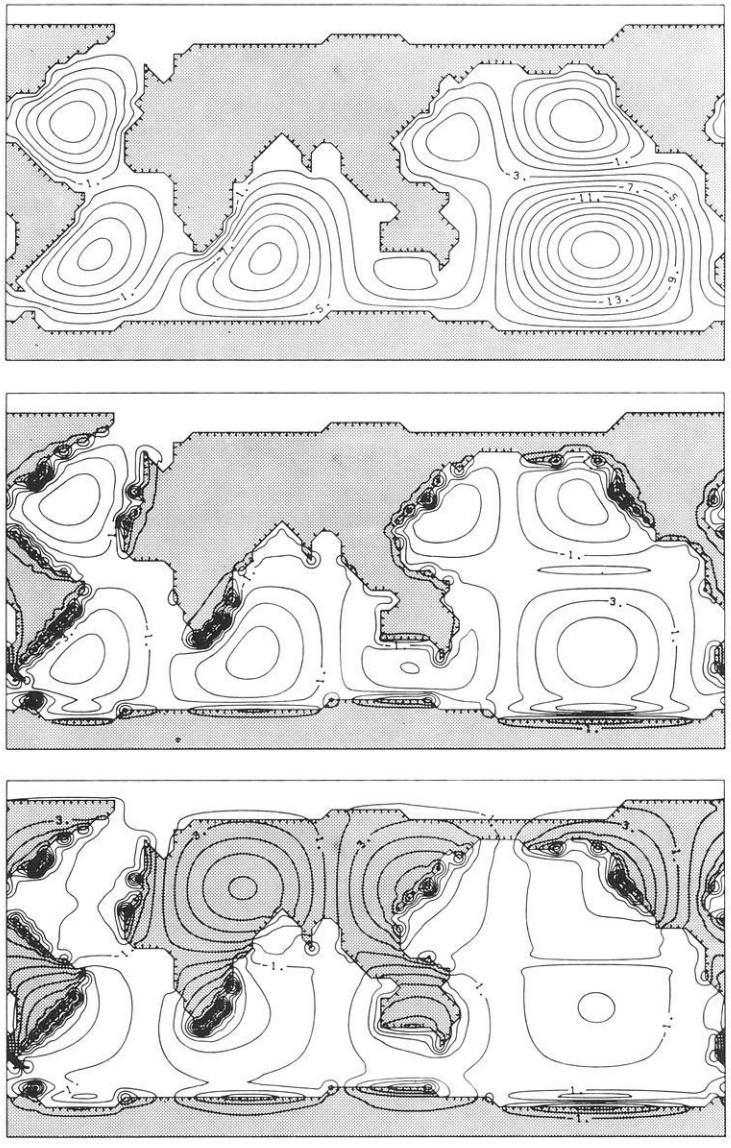

Fig. 4a–c. The in-phase part of the solution for induction by the unit amplitude harmonic $\sin 2\lambda P_3^2(\cos\theta)$ of period 12 h. Contour values as in Fig. 2. **a** Streamline function; **b** induced vertical field; **c** total vertical field

this is due to the low frequency of the inducing field and to the finite conductance of the oceans. It implies that all three terms in Eq. (1) are important. For high frequency (and/or high conductance) the term on the l.h.s. of Eq. (1) becomes relatively small and Z^e (which is real) is balanced by Z^i over the oceans. The part of Z^i in quadrature would then be small. Clearly a period of 24 h is not one of these 'high frequency' problems, but we begin to see these effects for periods of 12 and 8 h.

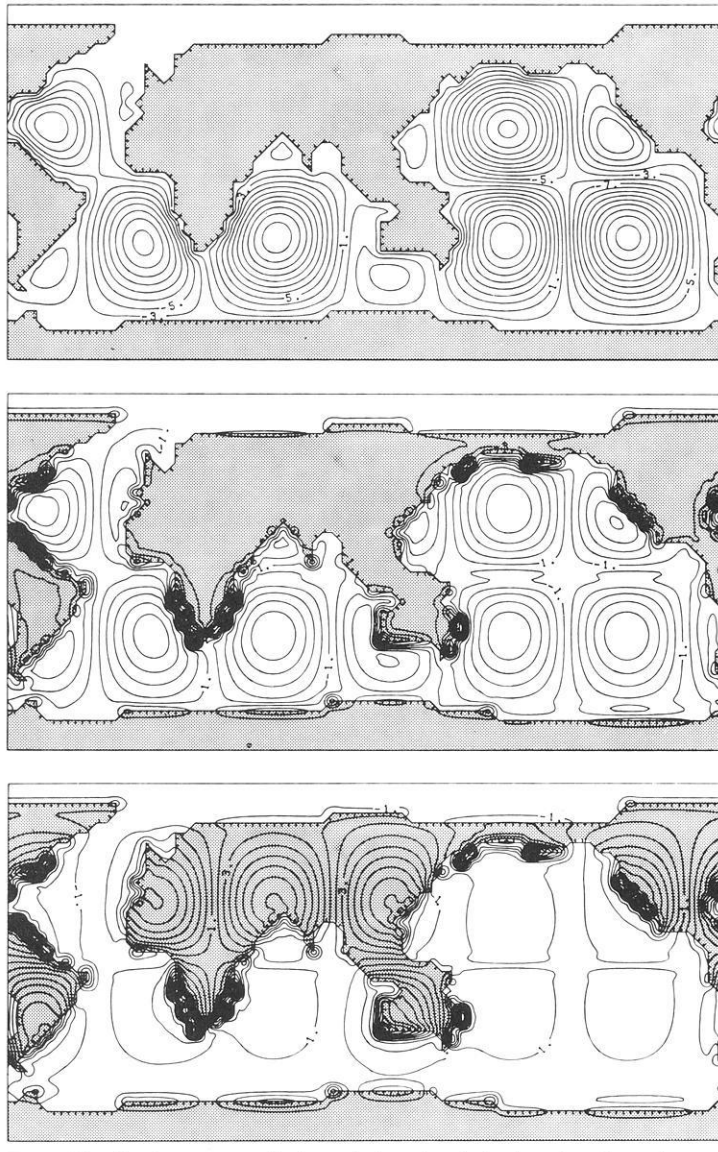

Fig. 5a–c. The in-phase part of the solution for induction by the unit amplitude harmonic $\cos 3\lambda P_4^3(\cos\theta)$ of period 8h. Contour values as in Fig. 2. **a** Streamline function; **b** induced vertical field; **c** total vertical field

Example: $\sin 2\lambda\, P_3^2(\cos\theta)$; In-Phase; Period 12 h

The relevant diagrams are shown in Fig. 4a–c. This harmonic has 8 vortices, 4 in the northern hemisphere and 4 in the southern hemisphere, with anti-symmetry about $\theta = 90°$. Figure 4a shows how the induced currents attempt to respond. The induced vertical field, Fig. 4b is more intense over oceans and ocean edges

Table 2. Spherical harmonic coefficients used to synthesise the external *Sq* field (extracted from Malin and Gupta, 1977, Table 2). The units are nT

k	n	m	AA^m_{nk}	BA^m_{nk}	AN^m_{nk}	BB^m_{nk}
1	1	1	0.49	−2.96	−4.73	−0.93
1	2	1	11.72	−0.53	−1.29	−9.72
1	4	1	−2.57	−0.51	−0.35	2.33
1	2	0	−0.17	−4.30	0.00	0.00
1	3	0	1.30	2.27	0.00	0.00
2	2	2	1.00	2.07	2.03	−0.69
2	3	2	−5.23	1.74	2.13	5.09
3	3	3	−1.39	−0.67	−0.61	1.04
3	4	3	1.65	−1.52	−1.68	−1.60

than the preceding two examples, and the result of this is seen in Fig. 4c. The total vertical field consists of the 8 vortices, but their strengths are greatly reduced over oceans and there is considerable distortion at ocean edges.

Example: $\cos 3\lambda\, P_4^3(\cos\theta)$; In-Phase; Period 8 h

The highest frequency in this set of examples corresponds to a period of 8 h. The spatial variation of the above harmonic results in 12 vortices, again anti-symmetric about $\theta = 90°$. The induced vortices can be seen in Fig. 5a for ψ, their strengths being dictated by the ocean distribution. The induced vertical field Z^i, Fig. 5b is now quite large over the oceans and their boundaries. Figure 5c shows dramatically the effect on the 12 vortices, their strengths being reduced over the oceans by about 80%. There is a clear progression, seen in Figs. 2c, 4c, and 5c leading towards the high frequency limit in which the in-phase total Z would be reduced to zero over the oceans. The boundary between a continent and an ocean is also that between the unaffected and the reduced vertical field variations. As the frequency increases, this boundary becomes more marked, hence the vertical field values there become more intense.

Application to the Sq Field During the IGY

The scalar magnetic potential for the external part of the field of the daily variations, $\mathrm{Sq}^{(\mathrm{ext})}$, may be written

$$\Omega^{(\mathrm{ext})}_{\mathrm{Sq}} = \mathrm{Re}\{a \sum_{n,m,k} (r/a)^n [(AA^m_{nk} - iBA^m_{nk}) \cos m\lambda + (AB^m_{nk} - iBB^m_{nk}) \sin m\lambda]\, P^m_n(\cos\theta) \exp(ik\alpha t) \tag{26}$$

where t is universal time in seconds and $\alpha = 2\pi/86{,}400$. Many analyses have derived the coefficients AA, AB, BA, and BB for various data sets. A recent analysis for the IGY is given by Malin and Gupta (1977) and we have selected

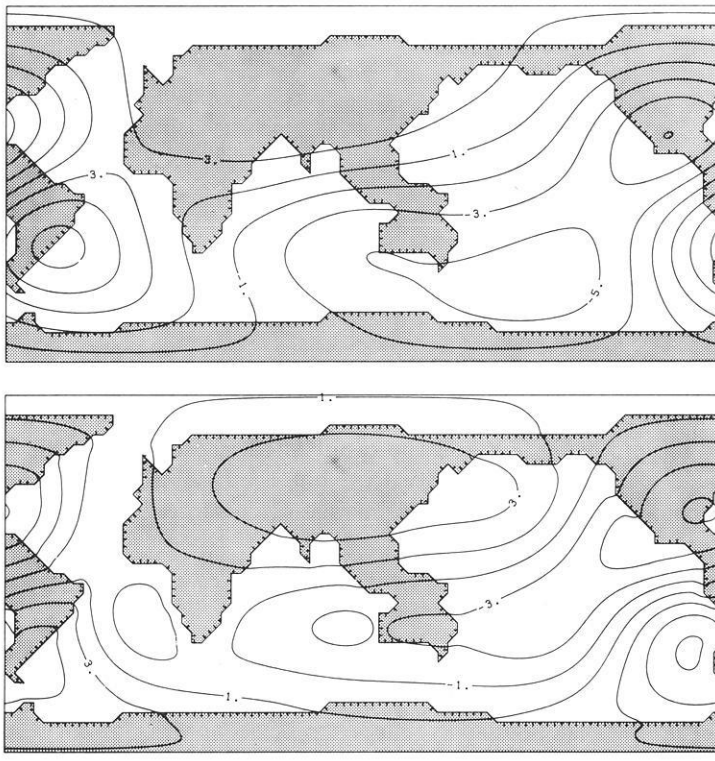

Fig. 6a and b. Equivalent current function for the internal part of *Sq* at universal time $T=16$h. **a** From observations analysed by Malin and Gupta (1977). **b** Calculated, 20 kA flows between adjacent contours

the most important terms to synthesise the $Sq^{(ext)}$ field, i.e., those with the largest coefficients bearing in mind the arguments following Eq. (25) concerning Z^e. The coefficients used, extracted from Malin and Gupta (1977) are given in Table 2.

To determine the response of our Earth/ocean conductivity model, the 16 solutions we have obtained are synthesised, with the $Sq^{(ext)}$ coefficients as weights, in the manner of Eq. (26). In common with previous descriptions of Sq, we present results in terms of an equivalent current system (Malin, 1973) at the surface $r=a$. For the calculated internal part of Sq, this equivalent current system has the streamline function

$$\psi^{(calc)}(t)=\mathrm{Re}(10^3/4\pi)\sum_{n,m,k}\{AA^m_{nk}-iBA^m_{nk})\,\tilde{\psi}^m_{nk,\cos} + (AB^m_{nk}-iBB^m_{nk})\,\tilde{\psi}_{nk,\sin}\}\exp(ik\alpha t) \tag{27}$$

where $\tilde{\psi}^m_{nk,\cos}$ and $\tilde{\psi}^m_{nk,\sin}$ are the equivalent current functions for solutions corresponding to the harmonics in (24). These equivalent current functions are composed of 3 parts, the streamline function for currents flowing in the oceans [e.g., $\psi^m_{nk,\cos}$; a solution to Eq. (1)], the equivalent current function for currents induced directly in the conductosphere by Z^p [e.g., $a((2n+1)/(n+1))\cdot\zeta^{2n+1}\cos m\lambda P^m_n(\cos\theta)$] and the equivalent current function corresponding

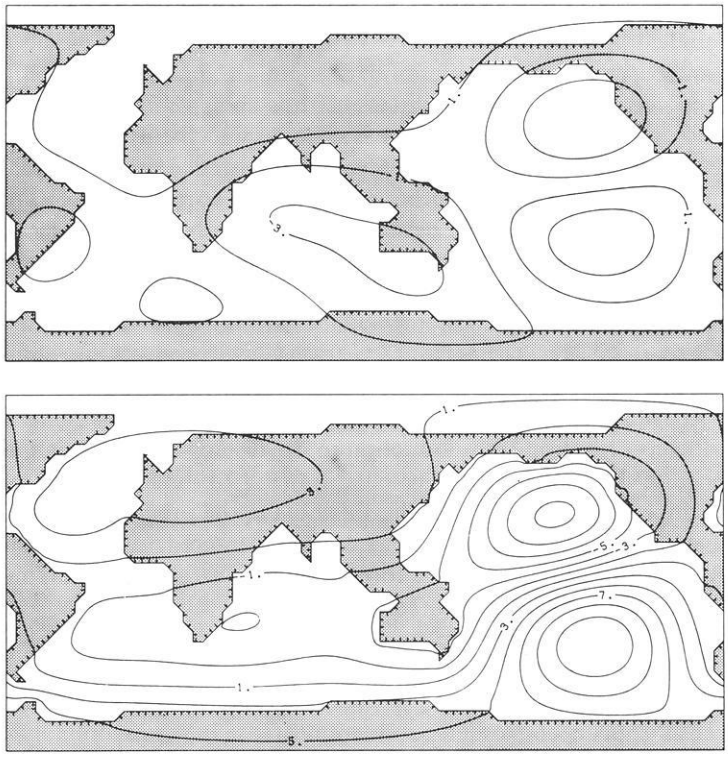

Fig. 7a and b. Equivalent current function for the internal part of *Sq* at universal time $T=20$ h. **a** From observations analysed by Malin and Gupta (1977). **b** Calculated, 20 kA flows between adjacent contours

to mutual induction between the oceans and conductosphere. A surface integral formula for this latter term may be derived using the methods of Hobbs and Price (1970) and is

$$\psi_A(\text{mutual}) = -\frac{1}{4\pi a^2} \iint_S \frac{\zeta(1-\zeta^4)}{(1+\zeta^4-2\zeta^2\cos\Theta)^{\frac{3}{2}}} \psi(\text{oceans})\, dS \tag{28}$$

where Θ is the angle between radius vectors to some point A and the integration point dS. Similarly, for a sine type harmonic the three terms are

$$\tilde{\psi}^m_{nk,\sin} = \psi^m_{nk,\sin} + a[(2n+1)/(n+1)]\, \zeta^{2n+1} \sin m\lambda\, P^m_n(\cos\theta) + \psi^m_{nk,\sin}(\text{mutual}). \tag{29}$$

In (27) we write $t=3600\,T$ so that T is universal time in hours.

The calculated part of Sq may be compared to that derived from the analysis of the observations given by Malin and Gupta (1977). They determine coefficients for the internal part of Sq, from which we may construct the equivalent current system

$$\psi^{(\text{obs})}(t) = \text{Re}(10^3\, a/4\pi) \sum_{n,m,k} [(2n+1)/(n+1)]\, \{(CC^m_{nk} - iDC^m_{nk}) \cos m\lambda + (CD^m_{nk} - iDD^m_{nk}) \sin m\lambda\}\, P^m_n(\cos\theta) \exp(ik\alpha t). \tag{30}$$

The coefficients used are those internal coefficients of Table 2 of Malin and Gupta (1977) labelled as $p=1$, $p=2$ and $p=3$ [in Eq. (30) above, $k \equiv p$].

A comparison between our calculations (27) and the observations (30) for two instants of universal time $T=16$ h and $T=20$ h is shown in Figs. 6 and 7. A numerical way of comparing the solutions is to compute the strengths of the current vortices. In Fig. 6, where the vortices are centred over America, the strengths of the main northern and southern hemisphere vortices are seen to be almost identical, the current flowing betweeen their foci being approximately 140 kA. In Fig. 7, when the vortices are centred over the Pacific Ocean, the strengths are very different and correspond to a current flow betweeen nothern and southern foci of 220 kA for the calculations but only 60 kA for the observations. These represent the best and worse cases, respectively, throughout the period of 24 h. Even in the best example, $T=16$ h Fig. 6, where the current strengths are the same, the current distribution is not. At this instant of universal time, the contribution from induction in the oceans is fairly small, even so, some influence of the oceans in the calculation (Fig. 6b) is evident from the displacement of the current foci towards the Pacific. On the other hand, $T=20$ h (Fig. 7) is a time at which the current vortices are centered over the Pacific Ocean, consequently the oceanic contribution should then be at its maximum. This is clearly so in the calculation, Fig. 7b, but the observations Fig. 7a, suggest the opposite effect, that in the presence of a large ocean, the currents decrease. Such an effect seems to have no physical basis. However the 'observations' are the result of a spherical harmonic analysis of magnetic fields measured predominantly over European and other continental areas. It seems unlikely that they could represent an effect seen only over the oceans and coastal regions. Further work is in progress using also other Sq analyses to see if they can be used in some way as a test of vertical component oceanic induction.

Conclusions

The main point of this paper is to show that it is now possible to solve, numerically, problems of electromagnetic induction in a thin non-uniformly conducting shell surrounding a conductosphere of perfect conductivity. The solutions are determined iteratively in only a few steps and can be obtained for any inducing field and frequency. For a 5° grid they are accurate to about 1 %. It should be noted that these are full solutions to the vertical component oceanic induction problem, as opposed to the simple outer solution approximation of Beamish et al. (1979).

Some of the solutions were used to synthesise the effect of induction by Sq, and a comparison was made between these calculations and observations. The comparison was poor and cannot be said to support the view that vertical component induction in the oceans is the important mode. However the behaviour of the 'observations' in oceanic regions seems to imply that Sq analyses are not useful in testing the appropriateness of thin sheet models.

It is hoped that the solutions will be useful in other applications. For example, a knowledge of the response function of the Earth, that is the ratio of internal to external parts for a given harmonic and frequency, has often been used to infer the Earth's conductivity profile with depth. Such analyses assume the Earth is radially symmetric, so that a given spherical harmonic in the external field induces only that harmonic of the same form within the Earth. This is no longer true when we account for the non-uniform oceans and the solutions we have obtained will be useful in examining the interrelations between the external and the internal hamonics.

Acknowledgements. This work was supported by the Natural Environment Research Council under grant GR3/2705 by means of which one of us (G.J.K.D.) was funded. Edinburgh University provided full computing facilities. The paper was presented at the Fourth I.A.G.A. Workshop on Electromagnetic Induction, Murnau, Germany, September 1978. We would like to thank Dr. W.D. Parkinson for his valuable comments whilst a Senior Visiting Research Fellow in our Department.

References

Beamish, D., Hewson-Browne, R.C., Kendall, P.C., Malin, S.R.C., Quinney, D.A.: Induction in arbitrarily shaped oceans IV: *Sq* for a simple case. Geophys. J.R. Astron Soc. in press, 1979

Bullard, E.C., Parker, R.L.: Electromagnetic induction in the oceans. In: The sea, Vol. IV, Ch. 18, 1970

Cuthill, E.H., Varga, R.S.: A method of normalised block iteration. J. Assoc. Comput. Mach. **6**, 236–244, 1959

Hobbs, B.A.: The calculation of geophysical induction effects using surface integrals. Geophys. J.R. Astron. Soc. **25**, 481–509, 1971

Hobbs, B.A., Brignall, A.M.M.: A method for solving general problems of electromagnetic induction in the oceans. Geophys. J.R. Astron. Soc. **45**, 527–542, 1976

Hobbs, B.A., Price, A.T.: Surface integral formulae for geomagnetic studies. Geophys. J.R. Astron. Soc. **20**, 49–63, 1970

Lahiri, B.N., Price, A.T.: Electromagnetic induction in non-uniform conductors, and the determination of the conductivity of the earth from terrestrial magnetic variations. Philos. Trans. R. Soc. London, Ser. A: **237**, 509–540, 1939

Malin, S.R.C.: Worldwide distribution of geomagnetic tides. Philos. Trans. R. Soc. London, Ser. A: **274**, 551–594, 1973

Malin, S.R.C., Gupta, J.C.: The Sq current system during the International Geophysical Year. Geophys. J.R. Astron. Soc. **49**, 515–529, 1977

Price, A.T.: The induction of electric currents in non-uniform thin sheets and shells. Q.J. Mech. Appl. Math. **2**, 283–310, 1949

Received June 5, 1979; Revised Version August 27, 1979